Supplementary Online Materials

Mutagenic conformation of 8-oxo-7,8-dihydro-2'-dGTP in the confines of a DNA polymerase active site

Vinod K. Batra, William A. Beard, Esther W. Hou, Lars C. Pedersen,

Rajendra Prasad, and Samuel H. Wilson

Supplementary Figures

Supplementary Tables

Supplementary Methods

Supplementary References

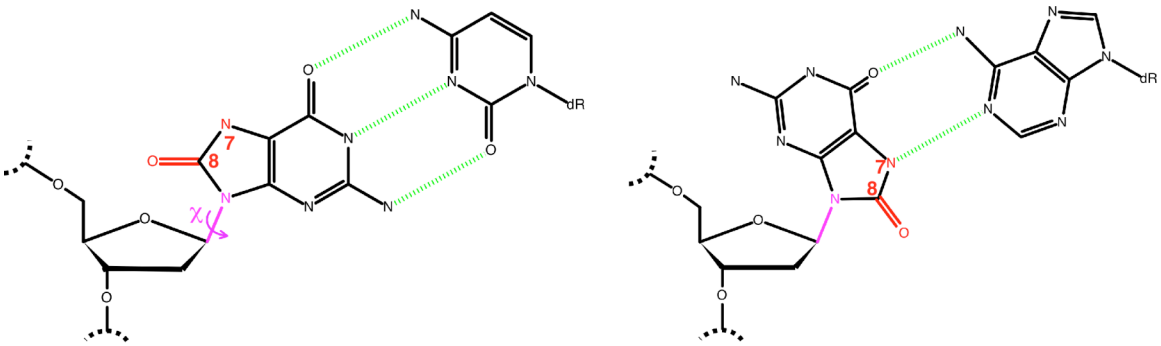

Supplementary Figure 1. Ambivalent coding potential of 8odG. In the *anti*-conformation, 8odG forms a Watson-Crick base pair with cytosine. Oxidation at C8 of guanine results in a carbonyl at C8 and protonation of N7 (red). This alters the hydrogen bonding capacity of the Hoogsteen edge of guanine converting N7 to a hydrogen bond donor that can base pair with adenine. Whereas the unmodified deoxyguanine glycosidic torsion angle preference is *anti*, χ (magenta), isolated 8-substituted purine nucleosides favor a *syn*-conformation due to steric repulsion between the deoxyribose and O8 of the modified purine base[1,2].

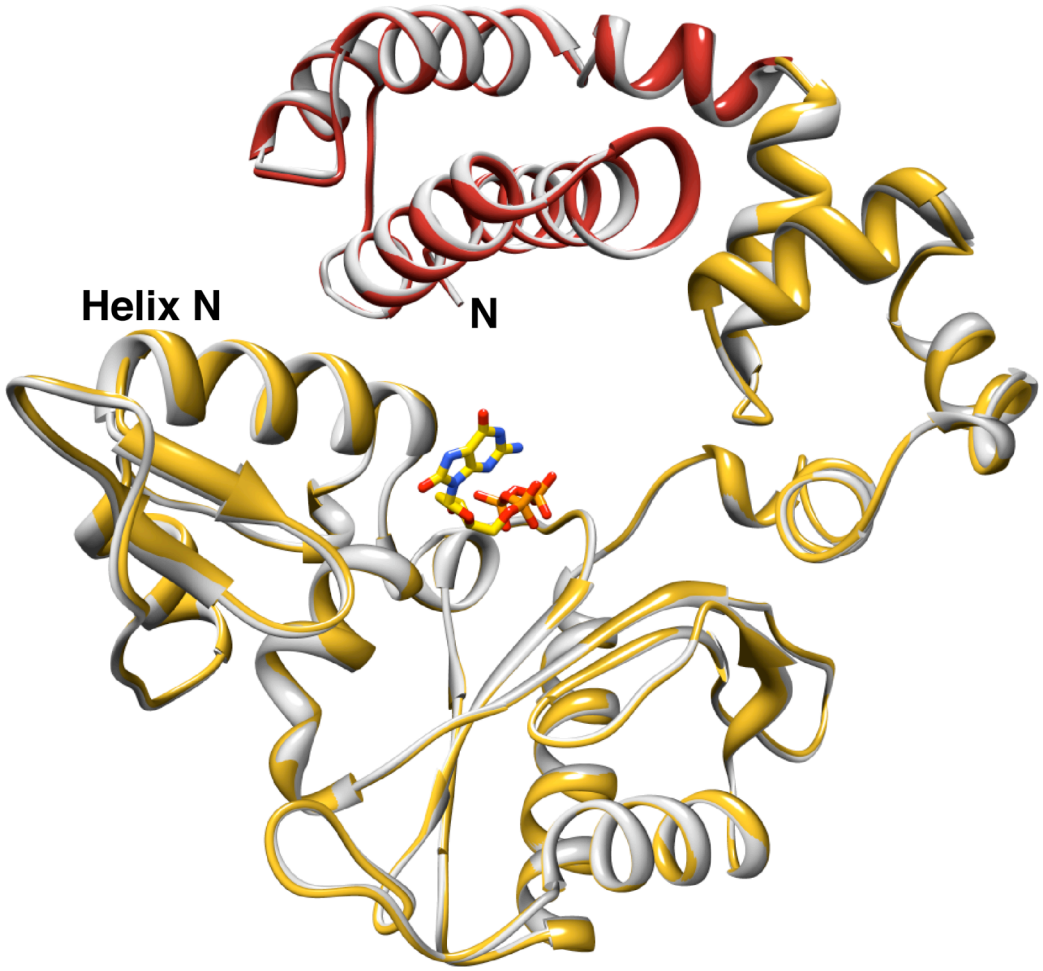

Supplementary Figure 2. Closed polymerase conformation with an active site 8odGTP–dA mismatch. DNA polymerase β DNA binary complex structures (i.e., without an incoming dNTP) are in an open conformation where α-helix N is positioned away from the nascent base pair binding pocket (not shown)[3]. The pol β backbone of the closed ternary substrate complex with a correct incoming nucleotide (gray ribbon, dUMPNPP; PDB ID 2FMS)[4] base paired with adenine is superimposed with the ternary complex with the 8odGTP—dA mismatch (gold/red ribbon). The two proteins superimpose with a root mean square deviation (rmsd) of 0.25 Å (all 326 Cαs) indicating that the polymerase is in a closed position with 8odGTP–dA in the nascent base pair binding pocket. The incoming 8odGTP (yellow carbons) of the mismatch structure is shown, but the DNA is omitted for clarity. The amino terminus (N) of the lyase domain (red) is indicated.

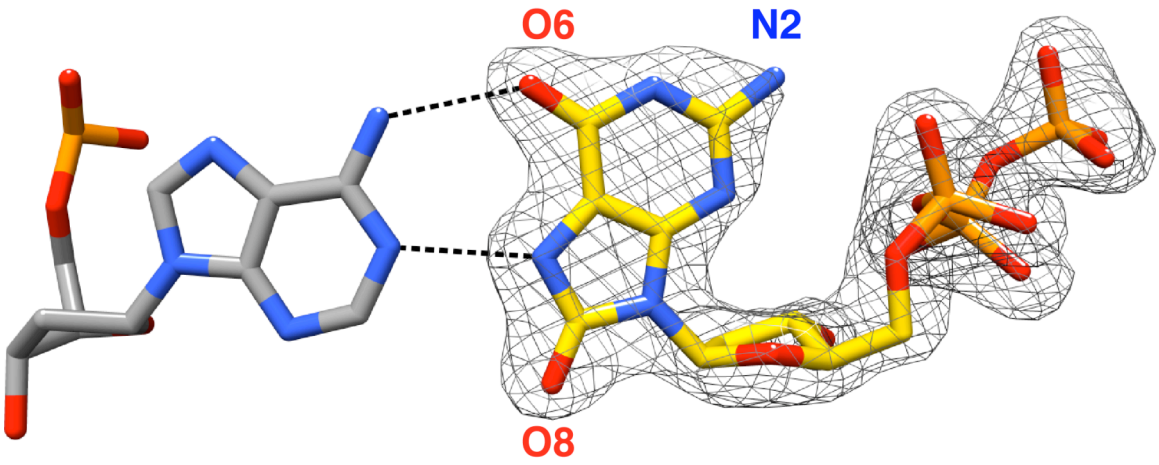

Supplementary Figure 3. *Syn*-conformation of 8odGTP. A F_o-F_c simulated annealing electron density omit map (gray) contoured at 4.0σ showing electron density corresponding to 8odGTP (yellow carbons). The templating nucleotide (dAMP) is also shown (gray carbons).

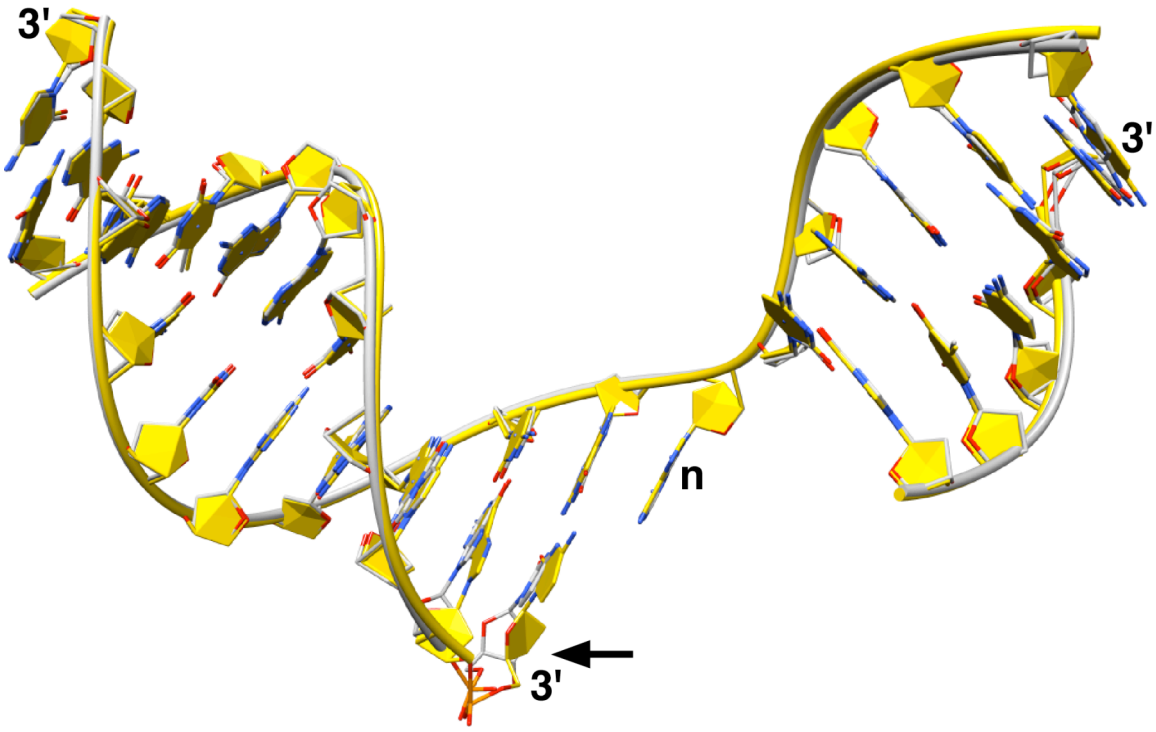

Supplementary Figure 4. Overall DNA conformation between matched and mismatched nascent base pairs is similar. The DNA backbone of the closed ternary substrate complex with a correct incoming nucleotide (gray carbons, dUMPNPP; PDB ID 2FMS)[4] base paired with adenine (n) is superimposed with the ternary complex with the 8odGTP—dA mismatch (yellow carbons). The phosphates superimpose with a rmsd of 0.42 Å. The 3´-end of each strand forming the gapped DNA is indicated. An arrow indicates the position of the distorted 3´-primer terminus of the ternary complex with 8odGTP. The incoming nucleotides are omitted for clarity.

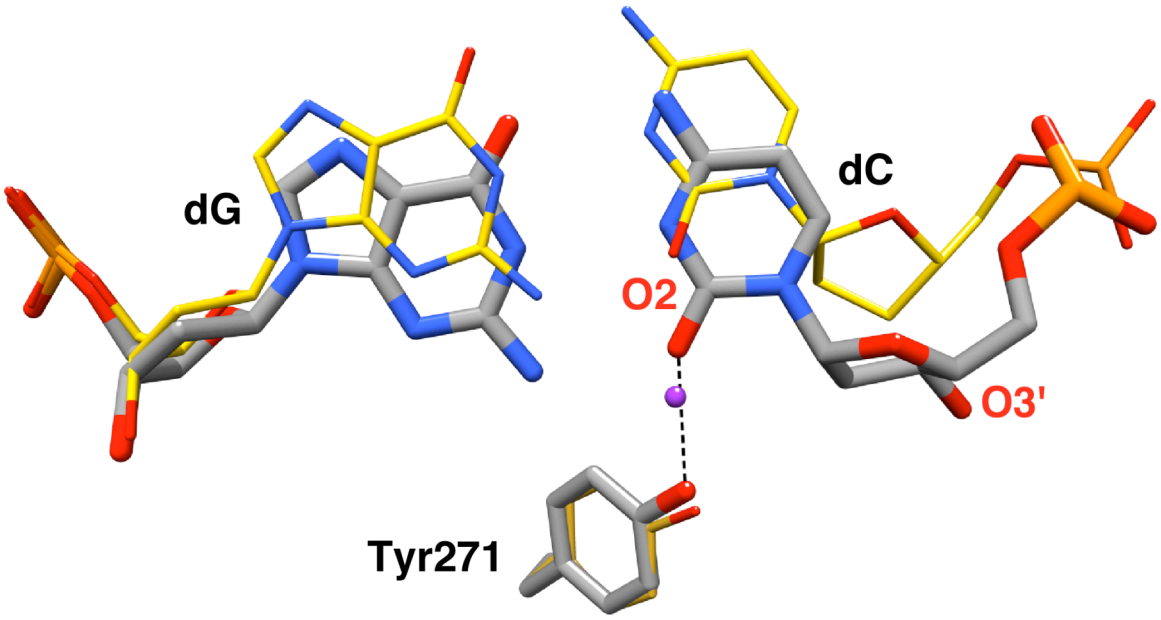

Supplementary Figure 5. Tyr271 hydrogen bonds to the base of the primer terminus with a Watson-Crick nascent base pair. The closed ternary substrate complex with a correct incoming nucleotide (PDB ID 2FMS; gray carbons)[4] is superimposed with the ternary complex with the 8odGTP—dA mismatch (yellow or orange carbons). The primer terminus base pair (dG–dC) of the ternary complex with a correct incoming nucleotide (O3´ of the primer terminus is indicated) is compared to the position of the dideoxy-primer terminus with an incoming 8odGTP. With an incoming 8odGTP, the primer terminus has lost a direct interaction with Tyr271 and observed to be repositioned into the major groove. An intervening water molecule (purple ball) occupies the approximate position of O2 of the primer terminus with a correct incoming nucleotide.

Supplementary Table 1. Preferential insertion of 8odGTP opposite a templating adenine (dA)

		dC[a]	8odGTP[b]	
DNA Polymerase	Family	dGTP/8odGTP	dA/dC	Reference
Bf–	A	6	13	5
Kf–	A	2,300	2	6
T7–	A	340,000	31	7
γ	A	10,000	37	8
α	B	490	0.2	5
II	B	320,000	0.04	7
ϕ29	B	2,010	0.3	9
III	C	35	1.3	10
β	X	1,300	11	11
λ	X	7,500	35	11
η	Y	120	185	12
HIV-1	RT	23,000	0.5	7

[a]Relative insertion efficiency opposite a template dC: $(\text{catalytic eff.})_{dGTP}/(\text{catalytic eff.})_{8odGTP}$. Accordingly, these numbers reflect how much 8odGTP insertion efficiency is decreased.

[b]Relative 8odGTP insertion efficiency: $(\text{catalytic eff.})_{dA}/(\text{catalytic eff.})_{dC}$. Values greater than one indicate a preference for insertion opposite dA. Although B-family DNA polymerases have an apparent preference for 8odGTP insertion opposite dC, insertion opposite dC is very poor.

Supplementary Table 2. Data collection and refinement statistics

	pol β–DNA–8odGTP
Data collection	
Space group	$P2_1$
Cell dimensions	
a, *b*, *c* (Å)	50.83, 80.03, 55.24
α, β, γ (°)	90, 107.7, 90
Resolution (Å)	50–2.00 (2.07–2.00)*
R_{merge}	0.062 (0.267)
$I / \sigma I$	18.7 (3.46)
Completeness (%)	99.3 (96.5)
Redundancy	3.5 (2.9)
Refinement	
Resolution (Å)	2.0
No. reflections	28427
R_{work} / R_{free}	19.0 / 24.6
No. atoms	
Protein	2611
Ligand/ion	669
Water	428
B-factors	
Protein	26.2
Ligand/ion	34.9
Water	36.6
R.m.s. deviations	
Bond lengths (Å)	0.005
Bond angles (°)	1.090

*Values in parentheses are for highest-resolution shell.

Supplementary Table 3. Contact distances between O8 of 8odGTP and the indicated atoms (see Figure 2b).

Residue, Atom	Distance (Å)
Primer terminus, C2´	3.00
8odGTP, C1´	2.95
8odGTP, C3´	3.25
8odGTP, C4´	3.26
8odGTP, O4´	2.69
8odGTP, O5´	2.53
8odGTP, P1	3.41

Supplementary Methods

Crystallization

Human pol β was over-expressed in *E. coli* and purified[13]. The DNA substrate consisted of a 16-mer template, a complementary 9-mer primer strand, and a 5-mer downstream oligonucleotide. Oligonucleotides were dissolved in 20 mM $MgCl_2$, 100 mM Tris-HCl, pH 7.5. Each set of template, primer, and downstream-oligonucleotides was mixed in a 1:1:1 ratio and annealed using a PCR thermocycler by heating 10 min at 90 °C and cooling to 4 °C (1 °C/min) resulting in a 1 mM mixture of two-nucleotide gapped DNA. The template, primer, and downstream DNA sequences were (5´—3´) CCG ACA GCG CAT CAG C, GCT GAT GCG, and GTC CC, respectively. The downstream oligonucleotide was 5´-phosphorylated. The annealed oligonucleotides were mixed with an equal volume of pol β and two-fold excess of ddCTP to create a dideoxy-terminated primer and a one-nucleotide gapped substrate with a templating adenine. Binary complex crystals were grown by vapor-diffusion sitting drop method at 18 ºC[4]. These crystals were then soaked in artificial mother liquor (50 mM imidazole, pH 7.5, 20% PEG-3350, 90 mM sodium acetate, 200 mM $MgCl_2$) and 2 mM 8odGTP (Jena Biosciences) and 12% ethylene glycol as cryoprotectant resulting in ternary complex crystals.

Data collection and structure determination

Data were collected at 100 K on a Saturn 92 CCD detector system mounted on a MiraMax®-007HF (Rigaku Corporation) rotating anode generator. Data were integrated and reduced with HKL2000 software[14].

Ternary substrate complex structures were determined by molecular replacement with a previously determined structure of pol β complexed with one-nucleotide gapped

DNA and incoming dUMPNPP (PDB ID 2FMS)[4]. These structures have similar lattices and are sufficiently isomorphous that molecular-replacement was not required. The model was refined and built using CNS[15] and O[16], respectively. The parameters and topology files for 8odGTP were prepared using the program XPOL2D[17]. The quality of the structure was assessed using Molprobity[18] (98.5% of residues in the favored range; 100% in the allowed range). The molecular graphics images were prepared in Chimera[19].

Supplementary References

1. Culp, S.J., Cho, B.P., Kadlubar, F.F. & Evans, F.E. *Chem. Res. Toxicol.* **2**, 416-422 (1989).
2. Uesugi, S. & Ikehara, M. *J. Am. Chem. Soc.* **99**, 3250-3253 (1977).
3. Beard, W.A. & Wilson, S.H. *Chem. Rev.* **106**, 361-382 (2006).
4. Batra, V.K. et al. *Structure (Camb)* **14**, 757-766 (2006).
5. Patro, J.N., Urban, M. & Kuchta, R.D. *Biochemistry* **48**, 8271-8278 (2009).
6. Purmal, A.A., Kow, Y.W. & Wallace, S.S. *Nucl. Acids Res.* **22**, 3930-3935 (1994).
7. Einolf, H.J., Schnetz-Boutaud, N. & Guengerich, F.P. *Biochemistry* **37**, 13300-13312 (1998).
8. Hanes, J.W., Thal, D.M. & Johnson, K.A. *J. Biol. Chem.* **281**, 36241-36248 (2006).
9. de Vega, M. & Salas, M. *Nucl. Acids Res.* **35**, 5096-5107 (2007).
10. Maki, H. & Sekiguchi, M. *Nature* **355**, 273-275 (1992).
11. Brown, J.A., Duym, W.W., Fowler, J.D. & Suo, Z. *J. Mol. Biol.* **367**, 1258-1269 (2007).
12. Shimizu, M. et al. *Biochemistry* **46**, 5515-5522 (2007).
13. Beard, W.A. & Wilson, S.H. *Methods Enzymol.* **262**, 98-107 (1995).
14. Otwinowski, Z. & Minor, W. *Methods Enzymol.* **276**, 307-326 (1997).
15. Brünger, A.T. et al. *Acta Crystallogr. D* **54**, 905-921 (1998).
16. Jones, T.A., Zou, J.Y., Cowan, S.W. & Kjeldgaard, M. *Acta Crystallogr. A* **47**, 110-119 (1991).

17. Kleywegt, G.J. & Jones, T.A. *Methods Enzymol*. **277**, 208-231 (1997).

18. Davis, I.W. et al. *Nucl. Acids Res*. **35**, W375-383 (2007).

19. Pettersen, E.F. et al. *J. Comput. Chem*. **25**, 1605-1612 (2004).